

**Photoelectron diffraction study of the low-temperature low-coverage oxygen layer on Rh(110)**

Federica Bondino,\* Giovanni Comelli, Alessandro Baraldi, and Renzo Rosei

*Dipartimento di Fisica, Università di Trieste, 34127 Trieste, Italy and Laboratorio TASC-INFN, 34012 Trieste, Italy*

Silvano Lizzit, Andrea Goldoni, Rosanna Larciprete,† Giorgio Paolucci

*Sincrotrone Trieste S.C.P.A., S.S. 14 Km 163.5, 34012 Trieste, Italy*

(Received 8 January 2002; revised manuscript received 2 May 2002; published 1 August 2002)

The local adsorption geometry of the low-coverage, short-range-ordered layer formed upon oxygen adsorption on the Rh(110) surface at 120 K has been quantitatively characterized by photoelectron diffraction measurements and multiple-scattering cluster calculations. The results of the structural analysis are compatible with a model where the oxygen atoms are located in the symmetric or slightly asymmetric short-bridge sites of the unreconstructed Rh(110) surface. O adsorption induces a small increase of the first substrate interlayer distance with respect to the relaxation of the clean Rh(110) surface.

DOI: 10.1103/PhysRevB.66.075402

PACS number(s): 61.14.Qp, 68.43.Fg, 79.60.Dp

**I. INTRODUCTION**

The interaction between oxygen and rhodium single-crystal surfaces has been widely studied in recent years as oxygen is an intermediate species in many reactions of practical and fundamental relevance involving rhodium as catalyst,<sup>1</sup> like, for example, CO oxidation, NH<sub>3</sub> oxidation and NO conversion to N<sub>2</sub>. In order to shed light on the factors that control the catalytic activity of Rh, it is important to identify the adsorption structure of the reaction intermediates, such as atomic oxygen. At low coverage, oxygen adsorption is always dissociative on any of the clean low-index Rh surfaces. The interaction of oxygen with the Rh(110) surface is particularly interesting because oxygen leads to a large variety of phases, depending on the preparation conditions.<sup>1-3</sup>

At low temperature (below 170 K) and low coverage [below 0.35 monolayers (ML)], oxygen atoms form an adlayer lacking of long-range order, hereafter referred to simply as the LTLC phase. The LTLC phase has been previously investigated by means of vibrational spectroscopy,<sup>4</sup> scanning tunneling microscopy,<sup>5</sup> (STM) and density functional theory.<sup>6,7</sup> (DFT) calculations.

High-resolution electron energy loss spectra from the LTLC phase<sup>4</sup> show a single vibrational mode at  $\approx 71$  meV, in the range of vibrational frequencies characteristic of both the threefold and twofold sites. Since the vibrational spectrum of the saturated O/Rh(110) phase, where the atoms are adsorbed in threefold sites,<sup>8</sup> is characterized by peaks at 45 meV and 63 meV, the 71 meV mode was tentatively assigned to oxygen in a long-bridge adsorption site.

The STM investigations found that in the LTLC phase oxygen atoms are arranged in domains which locally have (2 $\times$ 3) or *c*(2 $\times$ 6) periodicity. In particular, the STM images clearly showed that in this phase the oxygen atoms sit in pairs oriented along the [001] direction. The strong azimuthal ordering of the oxygen couples suggested the existence of a mobile molecular precursor to O<sub>2</sub> dissociation, with the O-O axis aligned in the [001] direction. On the basis of the STM images, the long-bridge site previously proposed for the oxygen atoms could be ruled out because the latter appeared to be aligned with the first layer close-packed Rh

rows. Due to the low corrugation along the Rh rows, the exact location of the oxygen atoms in this direction could not be determined, but the short-bridge site was proposed as the only compatible with the vibrational data.

A more detailed analysis of the STM images showed a further effect. The O-O distance in the [001] direction appeared to be always shorter than 3.8 Å (the distance between adjacent Rh rows), thus suggesting that the oxygen atoms are in asymmetric short-bridge sites, pointing towards the adjacent fcc threefold sites. Furthermore, this distance appeared to decrease with increasing oxygen coverage, ranging from  $3.3 \pm 0.4$  Å at  $\approx 0.1$  ML to  $2.5 \pm 0.2$  Å at  $\approx 0.35$  ML.

This result is intriguing, as *ab initio* DFT calculations predict a minimum energy configuration for oxygen in the perfect short-bridge adsorption sites.<sup>7</sup>

Since the interpretation of STM images as direct topographic maps of the surface is not generally straightforward,<sup>9,10</sup> an independent quantitative structural characterization of the LTLC phase by means of a surface crystallographic technique is required. An unambiguous determination of the local geometry is crucial in order to obtain a deeper understanding of the dissociation mechanism of the oxygen molecules on the Rh(110) surface.

The use of conventional low-energy electron diffraction intensity-voltage (LEED *I-V*) method is ruled out, as the LTLC phase does not have long-range order. The synchrotron radiation photoelectron diffraction (PED) method appears to be the ideal technique for this system, as it is known to have local structure sensitivity without requiring long-range order.<sup>11,12</sup> In the following we report on the structural characterization of the LTLC phase of oxygen on Rh(110) obtained using azimuthal scan PED combined with multiple-scattering calculations.

**II. EXPERIMENT**

The experiment was carried out at the SuperESCA beamline of ELETTRA.<sup>13</sup> O 1s photoemission spectra, obtained with 650 eV photons, were acquired using a double-pass 150 mm hemispherical electron energy analyzer,<sup>14</sup> equipped with a 96-channel detector.<sup>15</sup> Sample position was set automatically using a motorized VG manipulator with five degrees of freedom. The base pressure in the ultrahigh-vacuum chamber during the experiments was always below  $2 \times 10^{-10}$  mbar.

The Rh(110) surface was cleaned by repeated cycles of  $\text{Ar}^+$  ion bombardment, annealing to 1200 K, oxygen exposure and reduction in hydrogen, until the surface exhibited a sharp  $(1 \times 1)$  LEED pattern and no impurities were detected by x-ray photoemission spectroscopy (XPS). Oxygen was dosed on the sample at 120 K by backfilling the chamber.

Several azimuthal angle PED scans were measured from layers with different oxygen coverage, in the 0.24–0.36 ML range. The photoelectron kinetic energy (127 eV) was such that surface sensitivity and backward scattering from the substrate were guaranteed. At the same time, the energy was high enough for the photoelectron scattering to be adequately described with the muffin-tin potential model. The intensity PED curves were obtained by measuring a O 1s photoemission spectrum at varying azimuthal angle and fixed emission angle and calculating the areas under the peaks after proper normalization and background subtraction. The procedure was repeated at different emission angles from  $17^\circ$  to  $59^\circ$  with respect to the surface normal.

In order to compare the experimental and the theoretical spectra, PED data were represented by a modulation  $\chi$  function defined as  $\chi = (I - I_0)/I_0$ , where  $I$  is the PED intensity and  $I_0$  is the average of  $I$  on the complete angular scan.

### III. RESULTS

A series of O 1s XPS spectra was taken during oxygen exposure up to saturation with an overall energy resolution of about 0.5 eV, in order to discriminate the different O adsorption species on the surface and to evaluate their coverage. Each XPS measurement took an average of 27 s.

Each photoemission spectrum was fitted with a sum of a linear background and one or two Doniach-Sunjic functions<sup>16</sup> convoluted with Gaussian functions. Oxygen coverage was evaluated from the peak areas after normalization and background subtraction. The O 1s XPS data of the uptake series can be fitted with a single peak up to a coverage of 0.36 ML. Thus, the low-coverage phase contains a single O adsorption state (O-I). Above 0.36 ML oxygen coverage, a second component (O-II) was needed, with  $\approx 0.5$  eV higher binding energy. Above 0.83 ML, the O-II state was the only species present on the surface.

Figure 1 shows the uptake curve resulting from the fitting procedure. The coverage of the O-I and O-II species is plotted versus  $\text{O}_2$  exposure at 120 K. The uptake is nearly identical to that measured after exposure at 270 K by Comelli *et al.*<sup>17</sup>

For the calibration of the coverage scale, the oxygen saturation coverage was set at  $\Theta = 1.0$  ML (achieved at a dose of  $\approx 10$  L), corresponding to a well-ordered  $(2 \times 1)p2mg$  phase on the unreconstructed surface.<sup>22</sup>

The experimental PED azimuthal data measured from a layer with  $\approx 0.32$  ML oxygen coverage are shown as lines with markers in Fig. 2.

Similar sets of PED curves were measured also for layers with  $\approx 0.24$  ML and  $\approx 0.36$  ML, in order to investigate the coverage-dependent variation of the O-O distance suggested by the STM results. Some small differences in the PED curves are indeed present, as shown in Fig. 3.

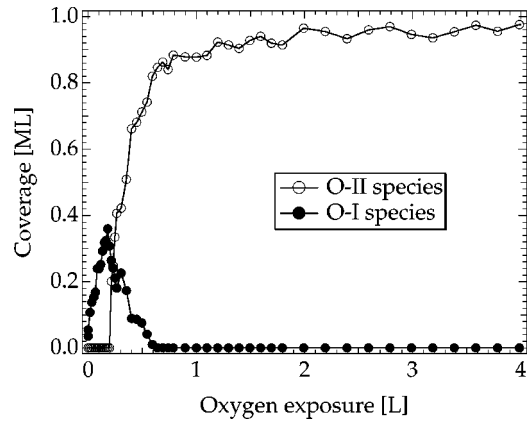


FIG. 1. O 1s uptake, taken at  $T = 120$  K with fast photoemission measurements. The lines between data point are guides to the eye.

### IV. CALCULATIONS

The extraction of structural parameters was performed by comparing the experimental PED data to the theoretical diffraction curves calculated for different trial structures, where the structural parameters were varied until the best agreement between simulated and experimental curves was obtained.

The PED simulations were performed using the MSCD photoelectron diffraction program package developed by Chen and Van Hove.<sup>18</sup> This code performs multiple-scattering cluster calculations based on the Rehr-Albers separable representation of the free propagator.<sup>19</sup>

Large semi elliptical clusters, consisting of 150–160 atoms, were used in all calculations. Convergence with respect to the multiple-scattering order, cluster size, maximum angular momentum, and Rehr-Albers approximation order was always checked. The finite acceptance angle ( $\pm 3^\circ$ ) of the analyzer and a correlated thermal vibrational factor<sup>19</sup> were also included in the calculations.

All phase shifts and radial matrix data were obtained by using the PSRM utility program<sup>20</sup> and providing appropriate muffin-tin potentials as input. These were calculated using programs from the Barbieri–Van Hove phase shift package.<sup>21</sup> A mean free path of 3 Å and an inner potential barrier of 8 eV were used in the best-fit simulations.

The overall agreement between the set of theoretical and experimental  $\chi$  functions was quantified by a multispectral reliability factor, evaluated over all the curves. The reliability factor we used is the one proposed by the Bradshaw-Woodruff group, defined as a normalized summation of the square deviations between the calculated,  $\chi_{cj}$ , and the experimental,  $\chi_{ej}$ ,  $\chi$  functions at the points  $j$  (Refs. 23 and 24):  $R_m = \sum_j (\chi_{cj} - \chi_{ej})^2 / \sum_j (\chi_{cj}^2 + \chi_{ej}^2)$ .

Different model structures were explored and optimized separately, always starting with structures having the oxygen atoms in high-symmetry sites. Specifically, structural models with O adsorbed either in long-bridge, on-top, short-bridge, and threefold fcc hollow sites were tested (see Fig. 4).

For each of these geometries, the vertical height of the O atom and the relaxation of topmost substrate layer were var-

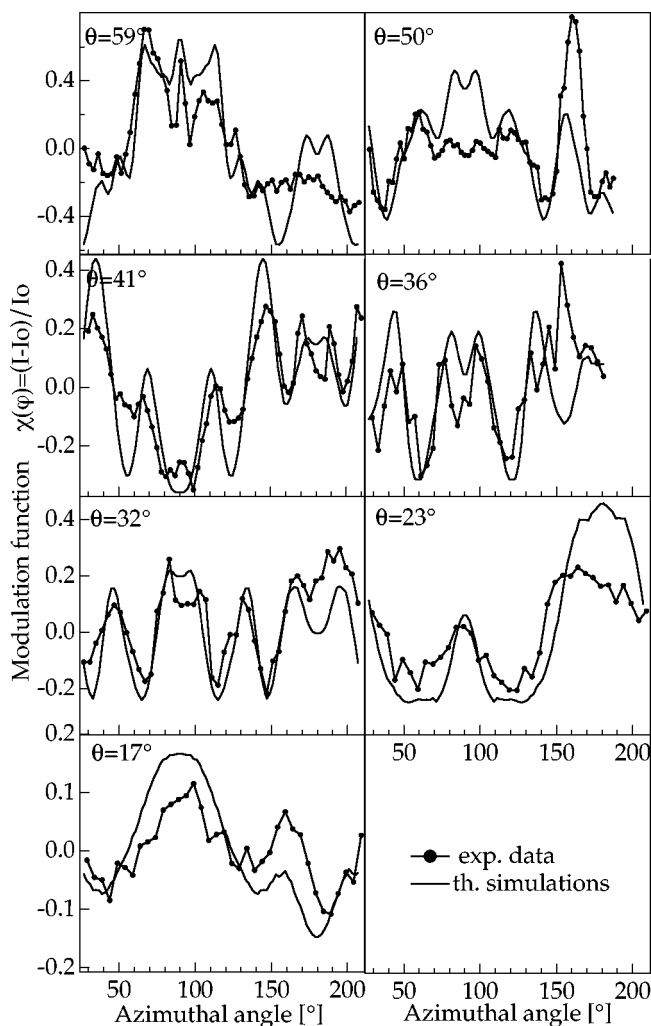


FIG. 2. Experimental (lines with markers) and calculated (straight lines) azimuthal PED curves of the O  $1s$  signal for an oxygen layer of 0.32 ML on Rh(110), measured at  $T=120$  K,  $KE=127$  eV, and different emission angles (from  $17^\circ$  to  $59^\circ$ ) from surface normal. The calculations correspond to the best-fit geometry (see text).

ied over a physically reasonable range. The best resulting reliability factors for each geometry are  $R_m=0.504$ , for long-bridge [Fig. 4(a)],  $R_m=0.496$  for on-top [Fig. 4(b)],  $R_m=0.171$  for short-bridge [Fig. 4(c)], and  $R_m=0.458$  for threefold adsorption site [Fig. 4(d)], respectively. This preliminary analysis clearly favored the short-bridge adsorption site. In a second step, the short-bridge adsorption configuration was further optimized to establish more subtle aspects of the structure. In particular, possible lateral displacements in the  $[001]$  direction of the O atoms from the position directly above the short-bridge site towards the adjacent fcc threefold sites; i.e., the asymmetric short-bridge adsorption configurations with oxygen atoms in pairs having a distance  $y_{OO}$  less than one lattice constant ( $3.80$  Å) were examined in order to investigate the model suggested by the STM analysis [see Fig. 4(d)]. Furthermore, a possible lateral reconstruction of the first layer Rh atoms was considered. The structural parameters which have been optimized are defined in Fig. 5:

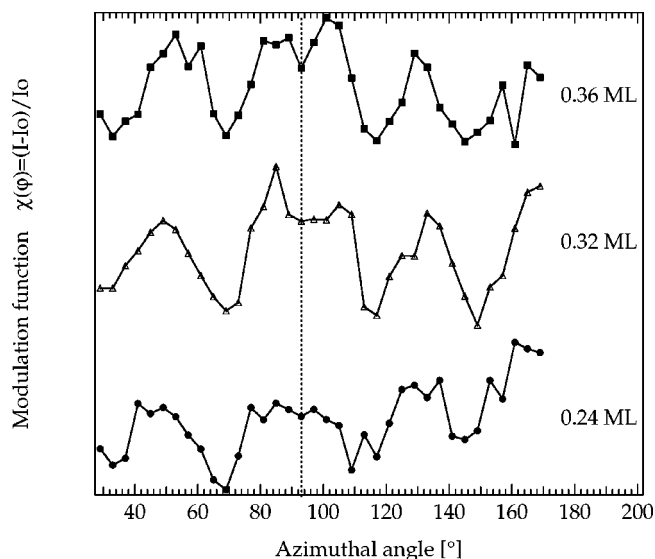


FIG. 3. O  $1s$  azimuthal PED curves, measured at the same kinetic energy ( $KE=127$  eV) and emission angle ( $\theta=32^\circ$ ), at different oxygen coverages. The lines between markers are guides to the eye.

the vertical height of the O atom above the surface,  $z_{ORh}$ ; the first to second Rh interlayer spacing  $d_{12}$ ; the second to third interlayer spacing,  $d_{23}$ ; the lateral distance  $y_{OO}$  between the oxygen atoms in the  $[001]$  direction; and the lateral distance  $y_{RhRh}$  between the first-layer Rh rows in the  $[001]$  direction.

The simulations have been obtained using a cluster in which the pairs of oxygen atoms are arranged in a  $(2 \times 3)$  periodicity, as suggested by the STM investigation.<sup>5</sup> The alternative  $c(2 \times 6)$  arrangement was also tested, yielding nearly identical PED curves, thus indicating that it is indeed the local structure around the emitting oxygen atoms [which is the same both in the  $(2 \times 3)$  and in the  $c(2 \times 6)$  arrangement] that mainly determines the diffraction curves.

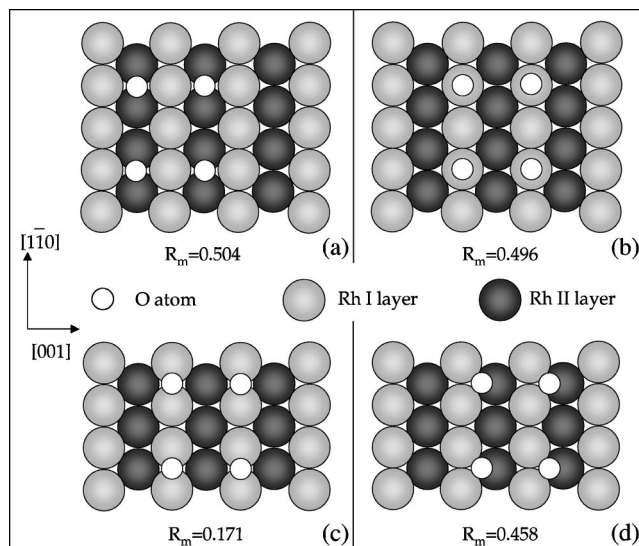


FIG. 4. Tested adsorption geometries and corresponding best-fit reliability factor values.

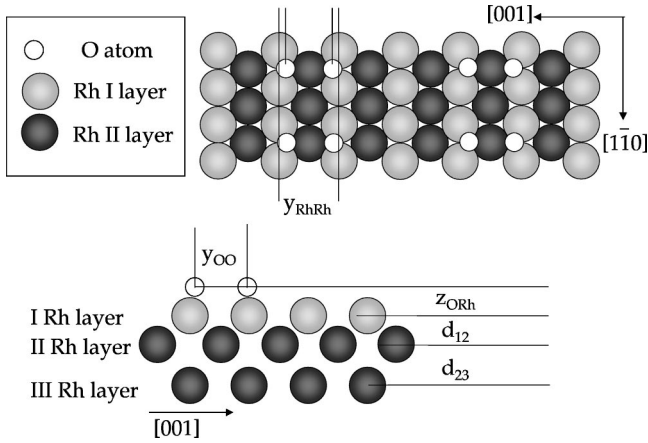


FIG. 5. Schematic model of the best-fit adsorption geometry formed by the oxygen pairs on the Rh(110) surface and definition of the structural parameters refined in the PED analysis.

The statistical errors associated with parameters were estimated by regarding all values giving structures with  $R$  factors lower than the sum of the  $R$  factor minimum  $R_{min}$  and its variance  $\text{Var}(R_{min})$  as falling within one standard deviation of the corresponding parameter value of the best-fit geometry.<sup>25,26</sup>

The variance in the minimum of the  $R$  factor was set equal to  $\text{Var}(R_{min}) = R_{min} \sqrt{2/N}$ , where  $N$  is the number of pieces of structural information contained in the PED modulation functions, as previously proposed.<sup>25,26</sup> We have adopted the criterion of considering  $N$  as the number of the actual experimental well-resolved peaks.

The calculated curves yielding the best  $R$  factor (multi-spectral  $R_m = 0.170$ ) are shown in Fig. 2 as lines superimposed onto the experimental PED data (lines with markers).

## V. DISCUSSION

The O  $1s$  binding energy shift between the O-I and O-II oxygen species clearly indicates that the LTLC phase involves an oxygen bonding configuration different from the  $(2 \times 1)p2mg$  phase, as already suggested by the vibrational data.<sup>4</sup>

Among the geometries tested in our simulations, best agreement with the 0.32 ML experimental PED data is obtained starting from the model shown in Fig. 4(c). The geometry favored by the  $R$  factor analysis is depicted in Fig. 5 and the associated structure parameters with the corresponding error bars are listed in Table I. In the resulting structure, the oxygen pairs are aligned along the  $[001]$  direction at near short-bridge sites, with a O-O distance along the  $[001]$  direction of  $3.7 \pm 0.25$  Å.

The best-fit adsorption configuration yielded  $R_m = 0.170$ , which is quite low for an adsorption system and therefore strongly supports the proposed geometry. The alternative models with oxygen adsorbed either on-top, threefold fcc, or in long-bridge adsorption sites of the Rh(110) surface can be safely ruled out, because they always gave  $R_m$  higher than 0.45, diverging significantly from the best-fit adsorption structure. It should be noted that the exact short-bridge ad-

TABLE I. Results of the PED analysis: best-fit parameters and error bars of the model with the minimum value of the  $R$  factor ( $R_m = 0.170$ ).

Parameter	value (Å)	error bar.
$y_{OO}$	3.70	$\pm 0.25$
$y_{RhRh}$	3.80	$\pm 0.1$
$z_{ORh}$	1.30	$\pm 0.05$
$d_{12}$	1.28	$\pm 0.05$
$d_{23}$	1.38	$\pm 0.05$

sorption geometry, predicted by DFT-LDA calculations,<sup>7</sup> yielded an  $R$  factor of 0.171, which is within the limits of our estimated standard deviation of  $R_m$  (0.041). Therefore, the results of the reliability factor analysis are compatible both with perfect short-bridge adsorption (O-O distance of 3.8 Å), or with a small lateral displacement ( $\approx 0.15$  Å) of the oxygen atom from the position directly above the short-bridge site.

We observe that the estimate of the  $y_{OO}$  parameter has the largest error bar, due to the uncertainty in the determination of the atomic coordinates parallel to the surface. However, it should be also pointed out that the PED results are not compatible with the O-O distance evaluated, at this coverage, on the basis of STM line profiles ( $2.7 \pm 0.2$  Å). In particular, the best-fit  $R_m$  values obtained for geometries with the O-O distance fixed at values below 2.9 Å were always above 0.60, which is out of the limits of our estimated confidence interval. This suggests that the local density of states imaged by STM does not reflect exactly the nuclear coordinates of the atoms, as was already observed, for example, in the case of the local structure around carbon atoms on Ni(100).<sup>10</sup>

From our analysis we obtain a vertical height of the O atom above the surface of  $1.30 \pm 0.05$  Å. This vertical spacing corresponds to a Rh-O bond length of  $1.87 \pm 0.05$  Å, identical, within the error bar, to the value ( $1.86 \pm 0.11$  Å) found for the  $(2 \times 1)p2mg-2O/Rh(110)$  structure by Batteas *et al.* in their LEED *IV* study.<sup>8</sup>

The first Rh-Rh interlayer distance appears to be contracted by 4.8% with respect to the bulk value. This corresponds to a slight *increase* of the first substrate interlayer distance with respect to the clean Rh(110) surface, which is contracted by 6.3%—7.8%.<sup>27,28</sup> If compared to the denser  $(2 \times 1)p2mg$  oxygen layer (1 ML), where the first interlayer contraction is 1.1%,<sup>8</sup> a roughly linear reduction of the first interlayer inward contraction as a function of the oxygen coverage can be obtained. This is an indication that the substrate surface participates actively in the chemisorption process, by optimizing the electronic environment for the O adatoms, via atom displacements. For O adsorption on this Rh(110) surface at a higher temperature, the atomic displacements are so massive that  $(1 \times n)$  missing row reconstruction occurs.<sup>1</sup>

A substantial displacement of the substrate metal atoms in the first layers due to oxygen adsorption is a quite common phenomenon, as reported, e.g., for the hexagonal fcc(111) and hcp(0001) surfaces.<sup>29,30</sup> In particular, for O on Ru(0001), a similar trend of a gradual, linear lifting of the contraction

of the mean topmost Ru spacing with O coverage was observed.<sup>31</sup>

A point to address is the influence of anisotropic vibrations of the emitter, which have not been accounted in our analysis. In particular, possible differences in the vibrational amplitudes in the [001], [1 $\bar{1}$ 0], and perpendicular directions could have an effect on the determination of the lateral shift away from the exact short-bridge position, although this effect should not be predominant at the low temperatures used for the present study.

A final point to discuss is the variation of the O-O distance with oxygen coverage that was proposed by the STM study. Although small differences are indeed observed in the PED curves measured for different coverages, they are in the limit of experimental uncertainties and do not allow a unique assignment of their origin to the variation of a specific structural parameter. Indeed the variations observed for decreasing O coverage (see Fig. 3) can be obtained in the PED simulations either by slightly varying the O-O distance along the [001] direction in the model structure or by slightly increasing the first interlayer spacing or the O-Rh vertical height. On this point therefore our PED data do not allow us to reach a definitive conclusion. In particular, we cannot rule out that the O-O distance varies as the oxygen coverage in-

creases (as suggested by STM), but we can definitively state that this variation, if present, is greatly overestimated by STM, which images the local density of states rather than the exact position of the oxygen atoms.

Moreover, even for the highest oxygen coverage of the LTLC phase where the O-O distance should be the shortest according to STM, PED results are compatible with the oxygen atoms positioned, within the error bars, in the symmetric short-bridge sites, as suggested by DFT calculations.

In conclusion, although the uncertainty in the determination of the distances parallel to the surface does not exclude a small displacement of the O atoms towards the adjacent fcc threefold sites, oxygen in the LTLC phase does not follow its tendency to adsorb on Rh surfaces in threefold sites,<sup>32</sup> but in this low-coverage regime it prefers short-bridge or nearly short-bridge adsorption sites.

## ACKNOWLEDGMENTS

We thank Y. Chen and M. Van Hove for providing us with the MSCD photoelectron diffraction calculation code. This work has been supported by INFN, by MURST under the program "COFIN01," and by Sincrotrone Trieste S.C.P.A.

\*Electronic address: bondino@tasc.infn.it

<sup>†</sup>Permanent address: ENEA, Divisione di Fisica Applicata, I-00044, Frascati, RM, Italy.

<sup>1</sup>G. Comelli, V.R. Dhanak, M. Kiskinova, K.C. Prince, and R. Rosei, *Surf. Sci. Rep.* **32**(5), 167 (1998).

<sup>2</sup>G. Comelli, V.R. Dhanak, M. Kiskinova, G. Paolucci, K.C. Prince, and R. Rosei, *Surf. Sci.* **270**, 360 (1992).

<sup>3</sup>V.R. Dhanak, G. Comelli, G. Cautero, G. Paolucci, K.C. Prince, M. Kiskinova, and R. Rosei, *Chem. Phys. Lett.* **188**, 237 (1992).

<sup>4</sup>D. Alfé, P. Rudolf, M. Kiskinova, and R. Rosei, *Chem. Phys. Lett.* **211**, 220 (1993).

<sup>5</sup>S.W. Hla, P. Lacovig, G. Comelli, A. Baraldi, M. Kiskinova, and R. Rosei, *Phys. Rev. B* **60**, 7800 (1999).

<sup>6</sup>K. Stokbro and S. Baroni, *Surf. Sci.* **370**, 166 (1997).

<sup>7</sup>G. Cipriani and S. Baroni (private communication).

<sup>8</sup>J.D. Batteas, A. Barbieri, E.K. Starkey, M.A. Van Hove, and G.A. Somorjai, *Surf. Sci.* **339**, 142 (1995).

<sup>9</sup>F. Besenbacher and I. Stensgaard, in *The Chemical Physics of Solid Surfaces*, edited by D.A. King and D.P. Woodruff (Elsevier, Amsterdam, 1994), Vol. 7, p. 573.

<sup>10</sup>R. Terborg, J.T. Hoeft, M. Polcik, R. Lindsay, O. Schaff, A.M. Bradshaw, R. Toomes, N.A. Booth, D.P. Woodruff, E. Rotenberg, and J. Denlinger, *Phys. Rev. B* **60**, 10 715 (1999).

<sup>11</sup>F. Bondino, G. Comelli, F. Esch, A. Locatelli, A. Baraldi, S. Lizzit, G. Paolucci, and R. Rosei, *Surf. Sci.* **459**, L467 (2000).

<sup>12</sup>D.P. Woodruff and A.M. Bradshaw, *Rep. Prog. Phys.* **57**, 1029 (1994).

<sup>13</sup>A. Abrami *et al.*, *Rev. Sci. Instrum.* **66**, 1618 (1995).

<sup>14</sup>A. Baraldi, and V.R. Dhanak, *J. Electron Spectrosc. Relat. Phenomen.* **67**, 211 (1994).

<sup>15</sup>L. Gori, R. Tommasini, G. Cautero, D. Giuressi, M. Barnaba, A. Accardo, S. Carrato, and G. Paolucci, *Nucl. Instrum. Methods Phys. Res. A* **431**, 338 (1999).

<sup>16</sup>S. Doniach and M. Sunjic, *J. Phys. C* **3**, 285 (1970).

<sup>17</sup>G. Comelli, A. Baraldi, S. Lizzit, D. Cocco, G. Paolucci, R. Rosei, and M. Kiskinova, *Chem. Phys. Lett.* **261**, 253 (1996).

<sup>18</sup>MSCD package by Yufeng Chen and Michel A Van Hove (<http://electron.lbl.gov/mscdpack/>).

<sup>19</sup>Y. Chen, F.J. García de Abajo, A. Chassé, R.X. Ynzunza, A.P. Kaduwela, M.A. Van Hove, and C.S. Fadley, *Phys. Rev. B* **58**, 13 121 (1998).

<sup>20</sup>PSRM code, Y. Chen and M.A Van Hove (private communication) (<http://electron.lbl.gov/mscdpack/>).

<sup>21</sup>A. Barbieri and M.A. Van Hove (private communication) (<http://electron.lbl.gov/leedpack/>).

<sup>22</sup>G. Comelli, V.R. Dhanak, M. Kiskinova, N. Pangher, G. Paolucci, K.C. Prince, and R. Rosei, *Surf. Sci.* **260**, 7 (1992).

<sup>23</sup>R. Dippel, K-U. Weiss, K.-M. Schindler, P. Gardner, V. Fritzsche, A.M. Bradshaw, M.C. Asensio, X.M. Hu, D.P. Woodruff, and A.R. González-Elipe, *Chem. Phys. Lett.* **199**, 625 (1992).

<sup>24</sup>Ph. Hofmann, K.-M. Schindler, S. Bao, V. Fritzsche, D.E. Ricken, and A.M. Bradshaw, *Surf. Sci.* **74**, 304 (1994).

<sup>25</sup>J.B. Pendry, *J. Phys. C* **13**, 937 (1980).

<sup>26</sup>N.A. Booth *et al.*, *Surf. Sci.* **387**, 152 (1997).

<sup>27</sup>F. Bondino, G. Comelli, A. Baraldi, S. Lizzit, A. Locatelli, F. Esch, A. Goldoni, R. Lariciprete, G. Paolucci, and R. Rosei, *Surf. Rev. Lett.* (to be published).

<sup>28</sup>F. Bondino, A. Baraldi, H. Over, G. Comelli, P. Lacovig, S. Lizzit, G. Paolucci, and R. Rosei, *Phys. Rev. B* **64**, 085422 (2001).

<sup>29</sup>U. Starke, M.A. Van Hove, and G.A. Somorjai, *Prog. Surf. Sci.* **46**, 305 (1994).

<sup>30</sup>H. Over, *Prog. Surf. Sci.* **58**, 249 (1998).

<sup>31</sup>D. Menzel, *Surf. Rev. Lett.* **6**, 835 (1999).

<sup>32</sup>A. Baraldi, J. Cerda, J.A. Martín-Gago, G. Comelli, S. Lizzit, G. Paolucci, and R. Rosei, *Phys. Rev. Lett.* **82**, 4874 (1999).